NUMERICAL CALCULATION OF ABLATION AND PLASMA EXPANSION INDUCED BY ELECTRIC BREAKDOWN OF SPACECRAFT INSULATOR SURFACE IN AMBIENT PLASMA ENVIRONMENT

Kouji Horikawa, Hirokazu Tahara and Takahisa Masuyama

Department of Mechanical Science and Bioengineering
Graduate School of Engineering Science, Osaka University
1-3, Machikaneyama, Toyonaka, Osaka 560-8531, Japan
Phone:+81-6-6850-6178
Fax:+81-6-6850-6179
E-mail:tahara@me.es.osaka-u.ac.jp

Abstract

In the future, LEO spacecraft will be larger and higher powered. Because of the balance of leakage currents through ambient space plasma, their main conductive body will have a higher negative potential without plasma contactor operation. When spacecraft operate with a higher voltage, more intensive electric breakdown, i.e. arcing, is suspected to occur on the surface. In this study, unsteady physical processes inside an arc spot, such as ablation and heating of insulator, and plasma generation and acceleration etc, were studied using Computational Fluid Dynamics (CFD). Direct-Simulation-Monte-Carlo Particle-In-Cell (DSMC-PIC) plasma simulation was also carried out to examine influences of ambient space plasma on plasma expansion processes outside the arc spot. The calculated arc current increased with time; had a peak and then decreased. Inside the arc spot, the calculated plasma resistance rapidly decreased with time; was kept low level and jumped just before extinguishment of arc. As a result, the plasma resistance characteristics agreed with the arc current characteristics. The calculated ablation rate rapidly increased with time; had a peak and then gradually decreased, although the calculated arc spot diameter gradually increased with time. Furthermore, the calculated arc spot diameter gradually increased with initial stored energy, although it was smaller than experimental ones. Both the neutral particle number density and the electron number density were the highest near arc initiation and decreased with time. Both the number densities were relatively high inside the arc spot compared with those outside it. The temperature of insulator surface in contact with plasma rapidly increased up to 5000 K near arc initiation and gradually decreased to 4000 K. Outside the arc spot, neutral particles in addition to charged particles around spacecraft played an important role in expansion of arc plasma by intensive ionization near the arc spot. Accordingly, high voltage operation of LEO spacecraft might bring drastic degradation of insulator surface by arcing, depending on insulator material properties and ambient plasma conditions.

1. Introduction

Spacecraft are in a severe environment in space. Their surfaces are exposed to energetic and reactive particles, such as electrons, ions, protons and oxygen atoms and ultraviolet light, including particles exhausted from plasma thrusters, during space missions. The environmental effect plays a crucial role in determining the spacecraft's reliability and lifetime [1]. Although the number density of ions such as oxygen and nitrogen is smaller than that of atomic oxygen in LEO, electrostatic interactions between the surface materials and the ambient plasma, such as negative or positive sheath creation, and charging and arcing phenomena, frequently occur. The ions are accelerated in a negative potential sheath on a solar array; the current generated by the solar array is leaked by impact of the ions, and the solar array is still degraded by sputtering and arcing due to the collected ions [2],[3]. Accordingly, the environmental factors cause changes of chemical structures of spacecraft materials and their optical and/or electrical properties [4],[5]. In GEO satellites, it is well known that the electrical breakdown of negative charging on their insulating surfaces causes intensive damages in the systems. In plasma contactor operations, the negative charging is expected to be mitigated by ions attracted from the plasma, resulting in surface degradation as well as in cases with high voltage solar arrays [6]-[8]. The mechanism of the material degradation, the structure of electrical sheaths and the charging and arcing processes must be understood.

In Osaka University, the structure of an ion sheath created around a high voltage solar array and the degradation of surface materials near the array due to high energy ion bombardment have been investigated [2],[3],[5]. The mitigation of negative charging by plasma flow, i.e. the feature of plasma contactor operations, has also been studied [6]-[9].

In the future, LEO spacecraft will be larger and higher powered. Because of the balance of leakage currents through ambient space plasma, their main conductive body will have a higher negative potential without plasma contactor operation. When spacecraft operate with a higher voltage, more intensive arcing is suspected to occur on the spacecraft surface [10],[11].

In this study, unsteady physical processes inside the arc spot, such as ablation and heating of insulator, and plasma generation and acceleration etc, are studied using Computational Fluid Dynamics (CFD). Direct-Simulation-Monte-Carlo Particle-In-Cell (DSMC-PIC) plasma simulation is also carried out to examine influences of ambient space plasma on plasma expansion processes outside the arc spot.

2. Hazard of Drastic Destruction of Spacecraft Surface Materials by Arcing in Plasma Environment

In general, the spacecraft conductive body, as shown in Fig.1, has a negative potential, near solar array voltage, on potential of space plasma. It is called absolute negative charging. Then, positive charging occurs on an insulator of the spacecraft surface. The large insulator works as a capacitor with a high capacitance. As shown in Fig.2(a), if electric breakdown occurs between the spacecraft conductive body and space plasma, i.e. destruction of the insulator by arcing, arc currents flow through several paths until neutralization of charge is finished. As a result, the arc current flowing from space plasma to the arc point of the spacecraft conductive body, as shown in Fig.2(b), is very high because of the high capacitance of the insulator. The arcing is suspected to intensively degrade insulator materials of spacecraft surface, specially with a high voltage solar array. Furthermore, the arcing characteristics are considered to depend on feature of space plasmas near spacecraft surface because interaction between electrons extracted from the arc spot and the ambient space plasma is expected to occur [10],[11]. Intensive arcing is suspected to occur in some ambient plasma environment.

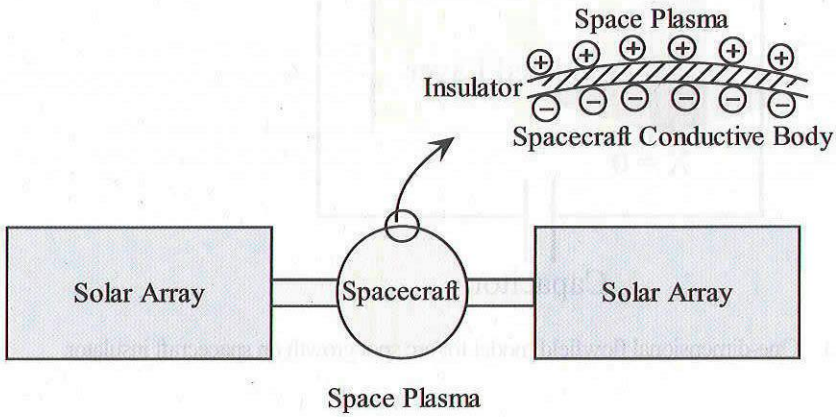

Fig.1 Feature of charging on spacecraft surface insulators.

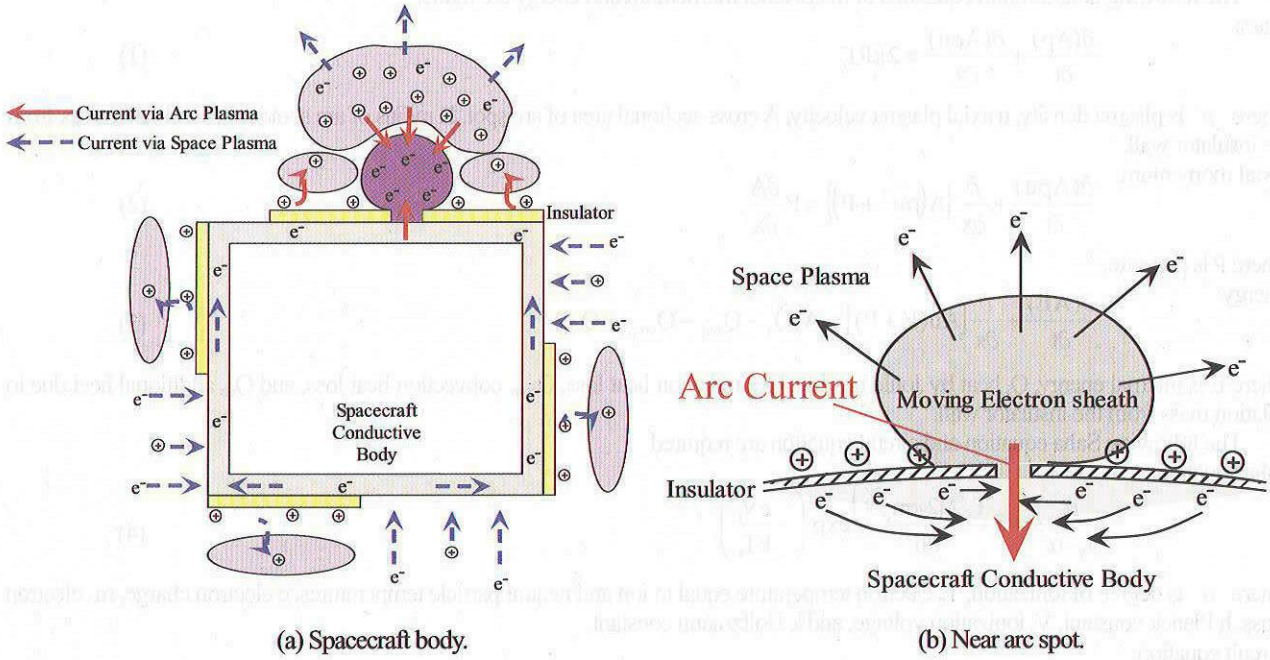

Fig.2 Current paths for arcing on surface insulator between spacecraft conductive body and space plasma.

3. Plasma Simulation

3.1 Arc Spot Growth Simulation by Computational Fluid Dynamics Code

Unsteady phenomena in an arc spot, such as ablation and heating of insulator, and plasma generation and acceleration etc, are

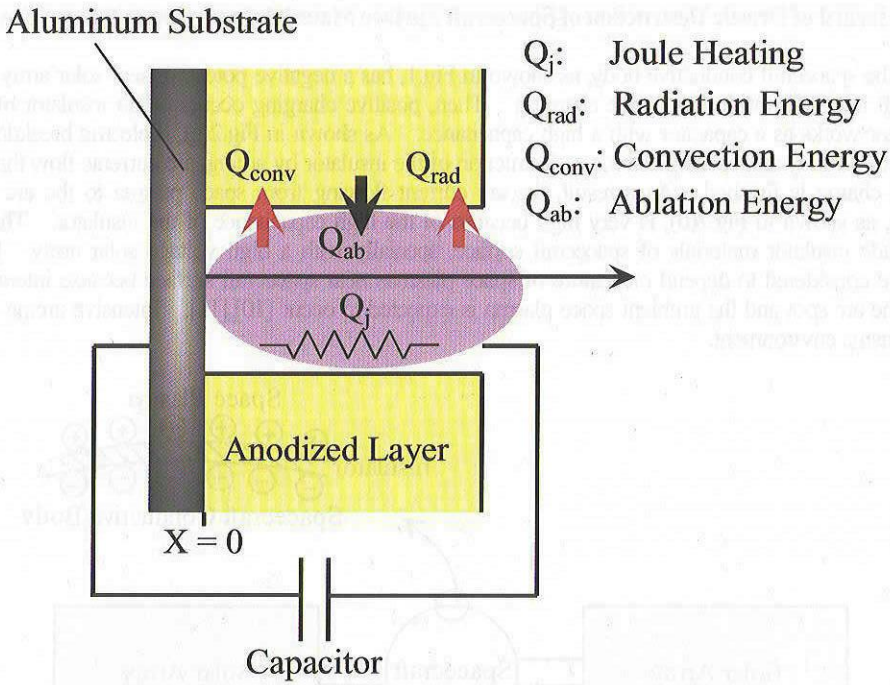

Fig.3 One-dimensional flowfield model for arc spot growth on spacecraft insulator.

numerically simulated using a one-dimensional fluid model. The calculation model, as shown in Fig.3, includes ionization under local thermodynamical equilibrium (LTE condition), ablation of the insulator wall, convection loss by electron, ion and neutral particle onto the wall, radiation loss from plasma, and heat conduction inside the insulator material.

The following conservation equations of mass, axial momentum and energy are made.

Mass:

$$\frac{\partial(A\rho)}{\partial t}+\frac{\partial(A\rho u)}{\partial x}=2\pi R\Gamma \tag{1}$$

where ρ is plasma density, u axial plasma velocity, A cross-sectional area of arc spot, R radius of arc spot and Γ ablation flux from the insulator wall.

Axial momentum:

$$\frac{\partial(A\rho u)}{\partial t}+\frac{\partial}{\partial x}\left\{A\left(\rho u^2+P\right)\right\}=P\frac{\partial A}{\partial x} \tag{2}$$

where P is pressure.

Energy:

$$\frac{\partial(AE)}{\partial t}+\frac{\partial}{\partial x}\left[Au(E+P)\right]=A(Q_j-Q_{rad}-Q_{conv}+Q_{ab}) \tag{3}$$

where E is internal energy, Q_j heat by Joule heating, Q_{rad} radiation heat loss, Q_{conv} convection heat loss, and Q_{ab} additional heat due to ablation mass from the insulator wall.

The following Saha equation and circuit equation are required.

Saha equation:

$$\frac{\alpha^2}{1-\alpha^2}=2\frac{T_e^{5/2}\left(2\pi m_e^{3/2}\right)}{Ph^3}\exp\left(-\frac{eV_i}{kT_e}\right) \tag{4}$$

where α is degree of ionization, T_e electron temperature equal to ion and neutral particle temperatures, e electron charge, m_e electron mass, h Planck constant, V_i ionization voltage, and k Boltzmann constant.

Circuit equation:

$$L_0\frac{d^2Q}{dt^2}+(R_0+R_p)\frac{dQ}{dt}+Q/C_0=0 \tag{5}$$

$$R_p=\int(\eta/A)dx$$

where L_0, R_0 and C_0 are inductance, resistance and capacitance, respectively, in electric circuit itself, Q electric charge, R_p plasma resistance, and η plasma resistance per unit area and unit length.

In energy equation (3), the heating and cooling terms are introduced as follows.

Joule heating:

$$Q_j = \eta j^2 \tag{6}$$

where j is axial current density.
Radiation cooling:

$$Q_{rad} = 1.57\times10^{-40}\, n_e^{\,2}\, T_e^{1/2} \tag{7}$$

where n_e is electron number density.
Convection cooling:

$$Q_{conv} = (q_e + q_i + q_n)\frac{2\pi R}{\pi R^2} \tag{8}$$

$$q_e = \varphi_e \cdot 2kT_e \tag{9}$$

$$q_i = \varphi_i \{2k(T_i - T_w) + e\phi\} \tag{10}$$

$$q_n = \varphi_n \cdot 2k(T_n - T_w) \tag{11}$$

where q_e, q_i and q_n are energy flux into cylindrical spot wall by electron, ion and neutral particle, respectively, ϕ_e ϕ_i and ϕ_n number flux by electron, ion and neutral particle, respectively, ϕ sheath voltage, T_i, T_n and T_w temperatures of ion, neutral particle and wall, respectively.

The wall sheath voltage and the number fluxes due to thermal motion are written as follows:

$$\phi = \frac{kT_e}{2e}\ln\left(\frac{T_e m_i}{T_i m_e}\right) \tag{12}$$

$$\varphi_i = \varphi_e = \frac{1}{4} n_e \left(\frac{8kT_i}{\pi m_i}\right)^{1/2} \tag{13}$$

$$\varphi_n = \frac{1}{4} n_n \left(\frac{8kT_n}{\pi m_i}\right)^{1/2} \tag{14}$$

where m_i is ion mass, and n_n neutral particle density.

The additional heat by ablated particles is represented as follows:

$$Q_{ab} = \Gamma / m_i \cdot 2kT_w \cdot \frac{2\pi R}{\pi R^2} \tag{15}$$

The number flux of ablated particles from the spot wall into plasma is as follows:

$$\Gamma = \alpha_v \left(\frac{m_i}{2\pi kT_w}\right) P_{vap} \tag{16}$$

$$\log P_{vap} = -T_c / T_w + P_c \tag{17}$$

where α_v is sticking coefficient, P_{vap} vapor pressure, and T_c and P_c characteristic temperature and pressure, respectively. In this calculation, a material of aluminum oxide (anodized aluminum) is used. The oxide thickness is 1.3 μm as well as those of Japanese Experimental Module in International Space Station. The values of α_v, T_c and P_c are 1.0, 27320 K and 11.296 Torr, respectively, and the plasma heavy-species particle is assumed to have the average mass of alumina atomic components. The value is m_i=3.4x10^{-26}kg, and the ionization voltage is assumed to be V_i=5.5 V.

At the boundary between the cylindrical spot wall and the plasma, the following energy relationship is needed:

$$\lambda \left.\frac{\partial T_w}{\partial r}\right|_{r=0} = (Q_{conv} + Q_{rad})\frac{\pi R^2}{2\pi R} - \Delta H \cdot \Gamma \tag{18}$$

where λ is thermal conductivity, and $\triangle$H energy for decomposition of alumina. The cylindrical unsteady equation of heat conduction is solved inside the alumina material. The exhaust plasma plume outside the arc spot is also modeled as divergent nozzle expansion without wall losses. The divergent half-angle is determined to be 20 deg.

Because it is difficult to model electrical breakdown of the insulator, a very small hole of 10 nm in diameter is located as the initial condition, and a low-density and low-temperature plasma (ρ=1.0x10^{3}kg/m^3, E=1.0x10^{3}J/m^3) is settled in the hole.

After all equations are normalized, the unsteady flowfield equations of (1), (2) and (3) are calculated by MacCormack scheme, and then the circuit equation (5) is solved under fixed flowfield condition by time step using the four-order Runge-Kutta method.

3.2 Plasma Expansion Simulation by Direct-Simulation-Monte-Carlo Particle-In-Cell Code

Direct-Simulation-Monte-Carlo Particle-In-Cell (DSMC-PIC) plasma simulation is carried out to understand features of plasma expanding from an arc spot on a spacecraft surface into the ambient plasma just after arcing. Figure 4 shows the two-dimensional calculation model. The calculation domain is 0.03 m x 0.03 m, and the grid number is 64x64. Electrons are injected from an arc spot on Y-axis corresponding to a spacecraft insulator surface. The width of the arc spot is assumed to be 2.36x10^{-5} m from the

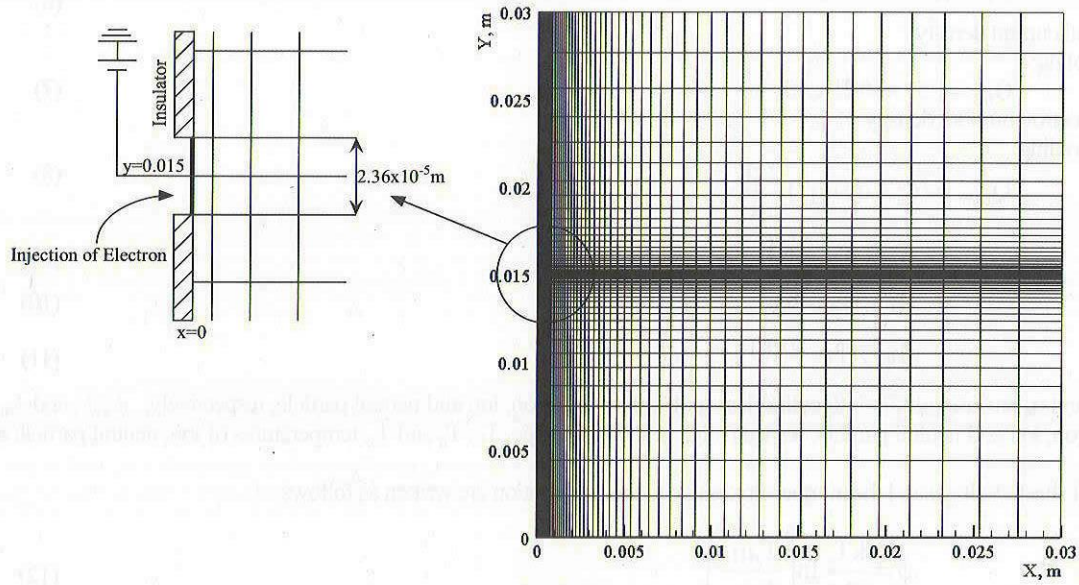

(a) Calculation domain.

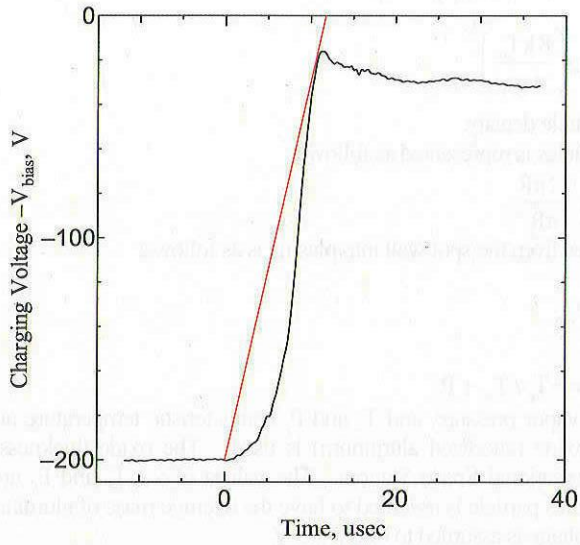

(b) Time variation in voltage applied at arc spot for calculation.

Fig.4 Two-dimensional model of Direct-Simulation-Monte-Carlo Particle-In-Cell (DSMC-PIC) simulation for electron-flow-induced plasma expanding from spacecraft surface into ambient plasma environment.

experimental data [10],[11]. As shown in Fig.4(b), the electrical potential of the arc spot is linearly applied in time, and then a constant electron charge of 2.0 Coulomb/sec is introduced from the arc spot. In the ambient plasma environment, there exist electrons, ions and neutrals. Both elastic and ionization collisions between electrons and neutrals are considered. Both electrons and ions move electrostatically. The kinetic equations of electron and ion, and Poisson's equation are governing ones, and Leap Flog scheme and Successive-Over-Relaxation method are used for their integrations. In boundary conditions, electric potential is zero on free boundaries in the ambient plasma, and its second-order derivative is zero on a solid boundary of the spacecraft insulator surface with the arc spot. Reflection of particles coming to the solid boundary is considered with assumption of conservation of energy and reflected angle independent of incoming angle.

4. Calculated Results and Discussion

4.1 Arc Spot Growth on Spacecraft Surface Insulator

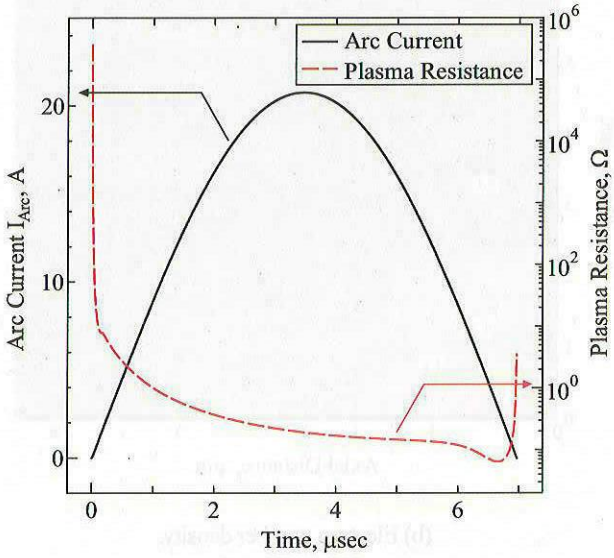

(a) Arc current and plasma resistance.

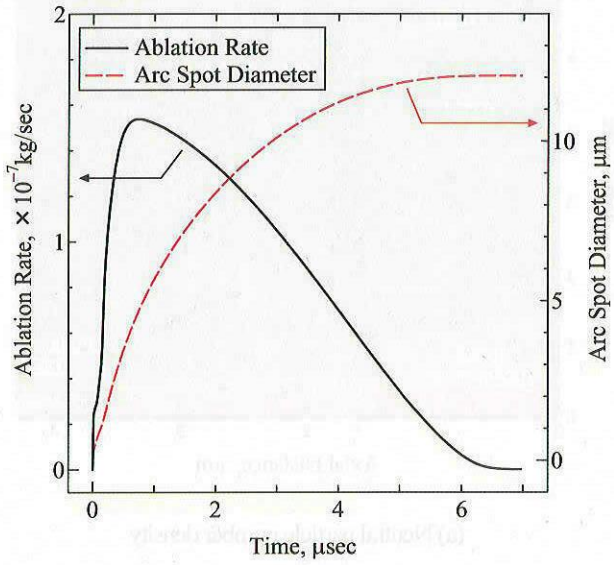

(b) Ablation rate and arc spot diameter.

Fig.5 Time variations of arc current, plasma resistance, ablation rate and arc spot diameter at an initial stored energy of 4.8 mJ.

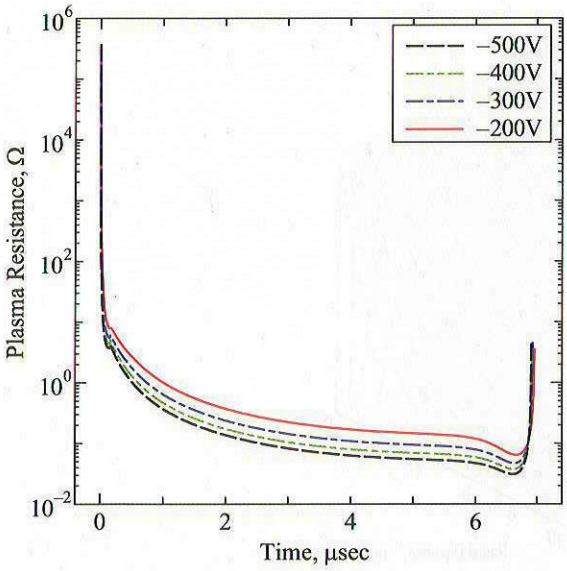

Fig.6 Time variations of plasma resistance dependent on energy initial charging voltage at a capacitance of 0.1 μF.

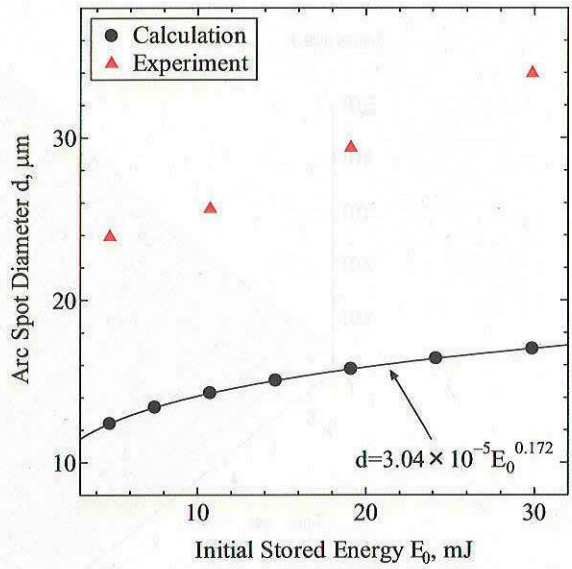

Fig.7 Calculated and measured arc spot diameter vs initial stored energy characteristics.

Figure 5 shows the time variations of arc current, plasma resistance, ablation rate and arc spot diameter at an initial stored energy of 4.8 mJ. The arc current increases; has a peak at 3.5 μsec and then decreases. The plasma resistance rapidly decreases; is kept low level and jumps just before extinguishment of arc. As a result, the plasma resistance characteristics agree with the arc current characteristics. The ablation rate, as shown in Fig.5(b), rapidly increases; has a peak at 1 μsec and then gradually decreases. On the other hand, the arc spot diameter gradually increases and almost does not change above 5 μsec.

Figure 6 shows the time variations of plasma resistance dependent on initial charging voltage at a capacitance of 0.1 μF [10],[11]. When the initial charging voltage changes from -200 to -500 V, the plasma resistance decreases in a wide range of time.

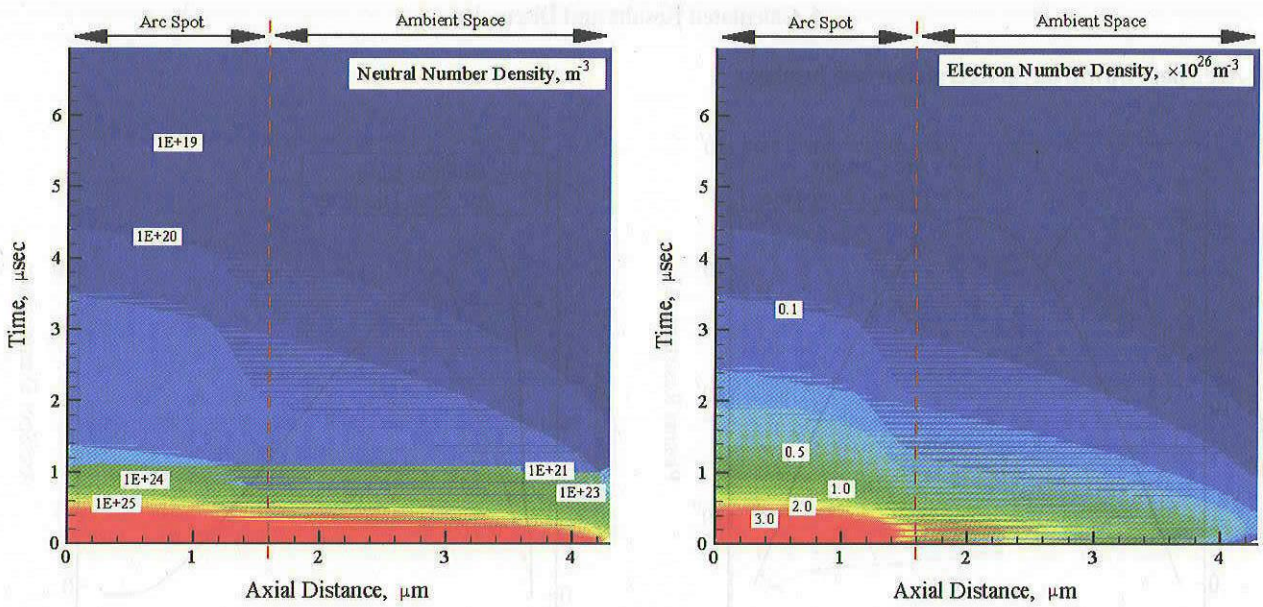

(a) Neutral particle number density. (b) Electron number density.

Fig.8 Axial variations of neutral particle number density and electron number density dependent on time at an initial stored energy of 4.8 mJ.

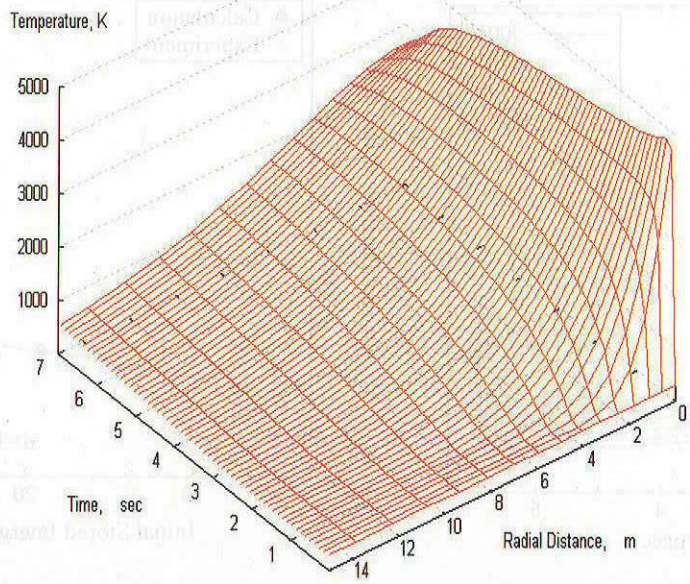

Fig.9 Time-dependent temperature distribution inside the insulator.

This is because plasma heating is enhanced as increasing initial stored energy. Accordingly, the calculated arc spot diameter, as shown in Fig.7, gradually increases with initial stored energy, and a fitting curve of $d=3.04\times10^{-5}E_0^{0.172}$ is obtained. However, the calculated spot diameters are smaller than experimental ones [10],[11]. We need improvement of the calculation model.

Figure 8 shows the axial variations of neutral particle number density and electron number density dependent on time at an initial stored energy of 4.8 mJ. Both the number densities are the highest near arc initiation and decreases with time. They are relatively high inside the arc spot compared with those outside it, and particularly the difference is large with electron number density. This is because of intensive ablation and Joule heating inside the arc spot and because of plasma expansion outside it.

Figure 9 shows the time-dependent temperature distribution inside the insulator. The temperature of insulator surface in contact with plasma rapidly increases up to 5000 K near arc initiation and gradually decreases to 4000 K. The temperature inside the insulator also increases to a few thousand K in a range of 0-10 μm.

4.2 Plasma Expansion Feature from Arc Spot on Spacecraft Surface

We examined the time variations of patterns of electron number density, ion number density and plasma potential at an initial arc spot potential of -200 V with an ambient plasma condition of plasma density 1.0×10^{13} m^{-3}, neutral particle density 1.0×10^{18} m^{-3} and electron temperature 2.0 eV [10],[11]. Electrons injected from the arc spot rapidly expanded. The ion number density increased toward the arc spot. This is mainly considered because of intensive ionization due to high-energy electrons near the arc spot and because of ions electrostatically attracted toward the arc spot. The plasma potential pattern agreed with those of electron and ion densities. From the plasma potential pattern, the electric field was very high near the arc spot and decreased outwards. The spatial change in plasma potential expanded up to 2 μsec because of drastic phenomena just after start of arcing, i.e. ionization, and rapid motions of electrons and ions, and after that the area became small.

We examined the patterns of ion density and plasma potential dependent on neutral particle number density at 8 μsec after start of arcing. There existed a high ion density region in front of the arc spot. When the neutral particle density increased, the area became large because of more intensive ionization. Then, a higher electric field was created near the arc spot although the area intensively concentrated near the arc spot.

Accordingly, the plasma expansion feature strongly depend on characteristics of ambient plasma, specially neutral particle number density.

5. Conclusions

Unsteady physical processes inside an arc spot created on spacecraft surface insulator due to electrical breakdown, such as ablation and heating of insulator, and plasma generation and acceleration etc, were studied using Computational Fluid Dynamics (CFD). Direct-Simulation-Monte-Carlo Particle-In-Cell (DSMC-PIC) plasma simulation was also carried out to examine influences of ambient space plasma on plasma expansion processes outside the arc spot. The calculated arc current increased with time; had a peak and then decreased. Inside the arc spot, the calculated plasma resistance rapidly decreased with time; was kept low level and jumped just before extinguishment of arc. As a result, the plasma resistance characteristics agreed with the arc current characteristics. The calculated ablation rate rapidly increased with time; had a peak and then gradually decreased, although the calculated arc spot diameter gradually increased with time. Furthermore, the calculated arc spot diameter gradually increased with initial stored energy, and a fitting curve of $d=3.04\times10^{-5}E_0^{0.172}$ was obtained. However, the calculated spot diameters were smaller than experimental ones. Both the neutral particle number density and the electron number density were the highest near arc initiation and decreased with time. Both the number densities were relatively high inside the arc spot compared with those outside it, and particularly the difference was large with electron number density. The temperature of insulator surface in contact with plasma rapidly increased up to 5000 K near arc initiation and gradually decreased to 4000 K. Outside the arc spot, neutral particles in addition to charged particles around spacecraft played an important role in expansion of arc plasma by intensive ionization near the arc spot. Accordingly, high voltage operation of LEO spacecraft might bring drastic degradation of insulator surface by arcing, depending on insulator material properties and ambient plasma conditions.

References

[1] NASA/SDIO Space Environmental Effects on Material Workshop, NASA CP-3035, 1989.
[2] H. Tahara, L. Zhang, M. Hiramatsu, T. Yasui, T. Yoshikawa, Y. Setsuhara and S. Miyake," Exposure of Space Material Insulators to Energetic Ions," J. Appl. Phys., Vol.78, No.6, pp.3719-3723, 1995.
[3] L. Zhang, T. Yasui, H. Tahara and T. Yoshikawa," X-ray Photoelectron Spectroscopy Study of the Interactions of O^+ and N^+ Ions with Polyimide Films," Jpn. J. Appl. Phys., Vol.36, No.8, pp.5268-5274, 1997.
[4] A.C. Tribble, R. Lukins, E. Watts, V.A. Borisov, S.A. Demidov, V.A. Denisenko, A.A. Gorodetskiy, V.K. Grishin, S.F. Nauma, V.K. Sergeev and S.P. Sokolova," United States and Russian Thermal Control Coating Results in Low Earth Orbit," J. Spacecraft and Rockets, Vol.33, No.1, pp.160-166, 1996.
[5] H. Tahara, K. Kawabata, L. Zhang, T. Yasui and T. Yoshikawa," Exposure of Spacecraft Polymers to Energetic Ions, Electrons and Ultraviolet Light," Nucl. Instrum. Methods, Vol.B121, pp.446-449, 1997.
[6] H. Tahara, T. Yasui and T. Yoshikawa," Space Plasma Simulator Performance Using an Electron Cyclotron Resonance Plasma Accelerator," Trans. Japan Soc. Aero. Space Sci., Vol.40, No.127, pp.59-68, 1997.
[7] D. Matsuyama, H. Tahara, T. Matsuda, T. Yasui and T. Yoshikawa," Ground Experiments of Interaction between Plasma Flow and Negatively Biased or Charged Materials," Proc. 26th Int. Electric Propulsion Conf., Kitakyushu, Japan, IEPC-99-224, pp.1314-1321, 1999.
[8] H. Tahara, T. Yasui, D. Matsuyama and T. Yoshikawa," Laboratory Simulation of Charging Relaxation by Plasma Flow," Proc. 7th Spacecraft Charging Technology Conf., ESTEC, Noordwijk, The Netherlands, ESA SP-476, 2001.
[9] H. Tahara, D. Matsuyama, T. Yasui and T. Yoshikawa," Mitigation Process of Spacecraft Negative Charging by Plasma Flow,"

27th Int. Electric Propulsion Conf., Pasadena, CA, USA, IEPC-01-258, 2001.
[10] T. Masuyama, M. Nagata, T. Onishi, H. Tahara and T. Yoshikawa," Ground Experiment and Numerical Simulation of Spacecraft Arcing in Ambient Plasma Environments," 8th Spacecraft Charging Technology Conf., Huntsville, AL, USA, 2003.
[11] T. Masuyama, M. Nagata, T. Onishi and H. Tahara," Ground-Based Experiment of Arcing on Spacecraft Insulator Surfaces in Ambient Plasma Environment," 24th Int. Symp. Space Technology and Science, Miyazaki, Japan, ISTS 2004-b-25, 2004.